PROCEEDINGS OF SCIENCE

Discovery of spin-modulated circular polarisation and radial velocity variations in the long-period intermediate Polar 1RXS J080114.6-462324

V. Moloi,[1,2,*] **S. B. Potter,**[2,3] **Z. N. Khangale**[1] **and P. A. Woudt**[1]

[1]*Department of Astronomy, University of Cape Town, Private Bag X3, Rondebosch 7701, South Africa*
[2]*South African Astronomical Observatory, PO Box 9, Observatory 7935, Cape Town, South Africa*
[3]*Department of Physics, University of Johannesburg, PO Box 524, Auckland Park 2006, South Africa*

E-mail: moloivick@gmail.com

We present a comprehensive phase-resolved photometric, spectroscopic, and polarimetric analysis of the intermediate polar (IP) 1RXS J080114.6–462324, based on multi-instrument observations. These include data from the HIgh speed Photo-POlarimeter (HIPPO), the Southern African Large Telescope (SALT), and the SAAO 1.0-m and 1.9-m telescopes, complemented by archival photometry from the Transiting Exoplanet Survey Satellite (TESS). The time-resolved spectroscopy reveals prominent emission features, including strong Balmer lines, most notably Hγ and Hβ, as well as He II λ4686, consistent with an actively accreting magnetic cataclysmic variable. In addition, we detect red-shifted absorption dips modulated on the white dwarf spin period, likely arising from infall within the magnetically channelled accretion curtains. We report the first detection of spin-modulated circular polarisation in this system, with a mean amplitude of $\sim$ +4%, observed independently in both photopolarimetric and circular spectropolarimetric data. The absence of Zeeman splitting and cyclotron harmonics constrains the magnetic field strength to $<$ 10 MG. We made the detection of the periodic signal at the lowest frequency of about 2.032 cycles d^{-1}, identified in both the TESS light curve and our spectroscopy, which is most likely to be the binary orbital frequency, placing 1RXS J080114.6–462324 among the intermediate polars with the longest known orbital periods.

High Energy Astrophysics in Southern Africa (HEASA2025)
16-20 September, 2025
University of Johannesburg, South Africa

*Speaker

 ISSN 1824-8039 . Published by SISSA Medialab.

PoS(HEASA2025)053

1. Introduction

Cataclysmic variables (CVs) are compact interacting binary systems consisting of a white dwarf (WD) primary accreting matter from a late-type, Roche-lobe–filling secondary star [1, 2]. In most CVs, mass transfer occurs via an accretion disc, however, in strongly magnetic systems, the WD's magnetic field can channel the accreting material along field lines or even suppress disc formation entirely. CVs are broadly classified into two categories: non-magnetic CVs, with magnetic field strengths $\lesssim 0.1$ MG (e.g., dwarf novae), and magnetic CVs, which include Intermediate Polars (IPs) and Polars.

Intermediate polar CVs are characterised by magnetic field strengths typically in the range 1-10 MG [3–5]. In these systems, the magnetic field is strong enough to truncate the inner regions of the accretion disc, and in at least one case (V2400 Oph) the system is entirely discless [6]. IPs are asynchronous systems, where the WD rotates faster than the binary orbit ($P_{\rm spin} < P_{\rm orb}$), typically with a spin-orbit ratio in the range $0.01 \lesssim P_{\rm spin}/P_{\rm orb} \lesssim 0.6$ [5, 7]. These systems often exhibit two dominant periodicities in their photometric and spectroscopic signals, one corresponding to the orbital period of the binary, and the other to the WD spin period.

1RXS J080114.6–462324, also known as PBC J0801.2–4625 was first detected as an X-ray source, and later classified as an intermediate polar CV based on its spectral characteristics, which includes strong Balmer emission, and strong He II [29]. This source has a WD spin period of about 1307.496 ± 0.024 seconds [16], and a suggested binary orbital period of 11.80989 ± 0.00048 hours. In addition, this system is also suspected to go through an outburst, possibly a *micronova* [19].

2. Observations and data reduction

A summary of photometric, spectroscopic, polarimetric, and circular spectropolarimetric observations obtained for 1RXS J080114.6–462324 are presented in Table 1.

Table 1: Log of photometric, spectroscopic, polarimetric, and circular spectropolarimetric observations

Date	Telescope	Instrument	Filter \Bandpass	Exposure (s)	Total time (hrs)
2017/04/03	1.9-m SAAO	SPUPNIC	4200–5400Å	200	5.50
2019/01/04	1.9-m SAAO	HIPPO	clear	–	5.60
2019/02/02–2019/02/27	TESS	TESS Photometer	6000–10000Å	120	591.30
2023/01/18–2023/02/12	TESS	TESS Photometer	6000–10000Å	120	610.20
2023/02/12–2023/03/10	TESS	TESS Photometer	6000–10000Å	120	617.10
2025/01/21	SALT	RSS	PC03850	300	0.58
2025/01/30	1.9-m SAAO	SHOCNWONDER	Clear	2	7.12
2025/01/31	1.9-m SAAO	SHOCNWONDER	r-filter	10	7.63
2025/02/01	1.9-m SAAO	SHOCNWONDER	g-filter	10	8.14
2025/02/02	1.9-m SAAO	SPUPNIC	4200–5400Å	200	7.73
2025/01/14–2025/02/11	TESS	TESS Photometer	6000–10000Å	120	666.54

The photometric data presented in this work were obtained with the South African Astronomical Observatory (SAAO) 1.9-m telescope, using the SHOCnWonder instrument. This dataset was reduced using the newly developed photometry pipeline IO_Phot[1].

In addition, we make use of the Transiting Exoplanet Survey Satellite (TESS) Pre-search Data Conditioning Simple Aperture Photometry (PDCSAP) data, which were extracted from the Mikulski Archive for Space Telescopes (MAST[2]). The TESS observations were obtained in the 6000–10000Å bandpass and provide complementary, continuous coverage that enhances the temporal sampling of the photometric variability.

Spectroscopic observations of 1RXS J080114.6–462324 were also acquired using the SAAO 1.9-m telescope, equipped with the SPUPNIC spectrograph [9], and employing the grating 4 setup, which has a dispersion of 0.62 (Å/pixel) [see, 10] . This data was reduced using standard procedures within the IRAF software package [11], which includes trimming, spectral extraction, wavelength calibration using arc-lamp exposures, and flux calibration.

Polarimetric observations were obtained with the HIgh-speed Photo-POlarimeter (HIPPO) (see, [12]) mounted on the SAAO 1.9-m telescope, using a clear filter. The polarimetric data obtained with HIPPO were reduced using the dedicated SAAO HIPPO reduction pipeline, developed in the C programming language and described in detail by [12].
Spectropolarimetric observations were obtained using the Southern African Large Telescope (SALT),

with the Robert Stobie Spectrograph (RSS) configured with the PG0900 grating. The SALT spectropolarimetric data were reduced using the PolSALT reduction pipeline [13–15] . The pipeline performs bias subtraction, flat-fielding, cosmic-ray removal, wavelength calibration, and extraction of the Stokes parameters from the modulated spectra.

3. Results

In this section we present some of our key findings and analysis on the target 1RXS J080114.6–462324.

3.1 Photometry

Figures 1 and 2 present the photometric light curves of 1RXS J080114.6–462324. The top panel of Figure 1 (TESS Sector 8) shows a pronounced increase in brightness, reported as an outburst, possibly a *micronova* [16]. The middle panel shows the combined light curve from Sectors 61 and 62, with an inset highlighting distinct brightness variations over time. The bottom panel presents the combined light curve from Sectors 88 and 89. Figure 2 shows the photometric observations obtained with the SAAO 1.9-m telescope, which exhibit clear short-term variability.

To search for any periodic signal, the TESS photometric light curves from Sectors 88 and 89 were further analysed using a Lomb–Scargle periodogram [22, 24], and the resulting periodogram is shown in Figure 3.

[1]IO_Phot is a Python-based pipeline for aperture photometry, developed at SAAO and is available at https://www.saao.ac.za/~sbp/IO_phot/IO_phot.py.

[2]MAST is a public NASA database providing calibrated light curves and data products from the TESS mission for exoplanet and time-domain astrophysics research.for more information see: https://archive.stsci.edu/missions-and-data/tess

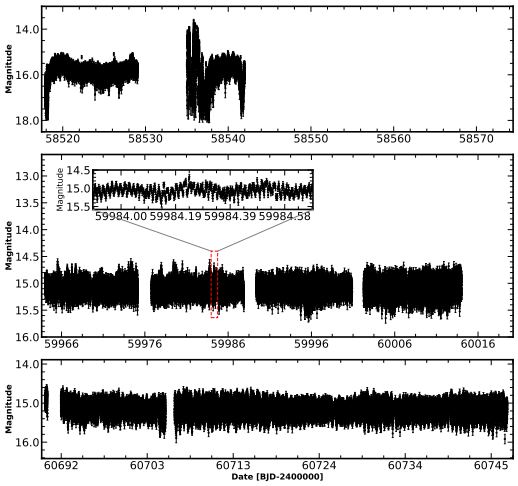

Figure 1: TESS PDCSAP light curves of 1RXS J080114.6–462324: **Top panel:** Sector 8; **Middle panel** Sectors 61–62; **Bottom panel** – Sectors 88–89. Adopted from figure 1 of [20]

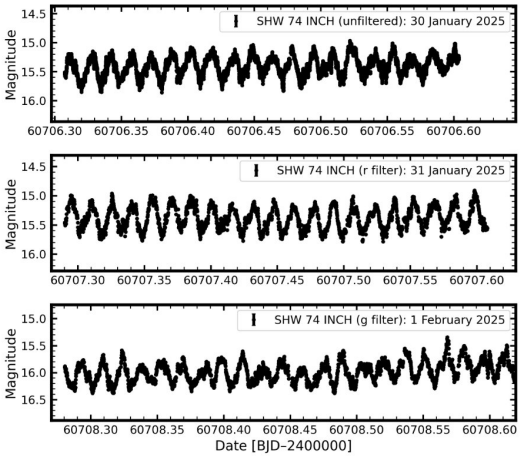

Figure 2: Photometric light curves of 1RXS J080114.6–462324 from the SAAO 1.9-m telescope. **Top:** Unfiltered data. **Middle:** r-band observations. **Bottom:** g-band observations.

The periodogram presented in Fig. 3 reveals four distinct periodic signals: two at lower frequencies (2.03 cycles d^{-1} and 4.06 cycles d^{-1}), and two at higher frequencies (66.08 cycles d^{-1} and 132.16 cycles d^{-1}). The signal at 2.03 cycles d^{-1} is attributed to the binary orbital frequency (Ω), corresponding to an orbital period of 11.8027 ± 0.0004 hours, with its first harmonic appearing at 2Ω. The signal at 66.08 cycles d^{-1} is associated with the spin period of the accreting WD, 1307.52 ± 0.05 seconds and we report this as the refined spin period, which is consistent with previously reported values [16–18].

The derived binary orbital period of 11.8027 ± 0.0004 hours places 1RXS J080114.6–462324 among the group of IPs with long orbital periods. The spin–orbit ratio of the system, $P_\omega/P_\Omega \approx 0.0307 < 0.1$, is consistent with a disc-fed accretion geometry [7, 21]. Using the refined WD spin period and the magnetic moment relation given in equation (21) of Patterson [5], we estimate the magnetic moment of the accreting WD to be $\mu \approx 2.47 \times 10^{33}$ G cm^3, which is consistent with the predicted range of magnetic moments for IPs [7, 21].

3.2 Spectroscopy

Figure 4 shows the optical average spectra of 1RXS J080114.6–462324 obtained with the SAAO 1.9-m telescope on 2017 April 3. This is a typical spectra of an Intermediate polar CV, showing strong Balmer emission lines (Hγ, Hβ) associated with accretion, along with helium lines He I λ4471 and He II λ4686 emission, the latter indicative of high-energy processes. A careful inspection of the optical spectra reveals the presence of red-shifted absorption dips, indicated by the arrow A, and B. These features are interpreted as absorption caused by the accretion curtains passing through the observer's line of sight, where material channeled along the WD's magnetic field lines partially obscures the emission from the accretion regions. Periodogram analysis further indicates that the appearance of these absorption features are modulated at the WD's spin period, consistent with a rotating magnetically confined accretion flow.

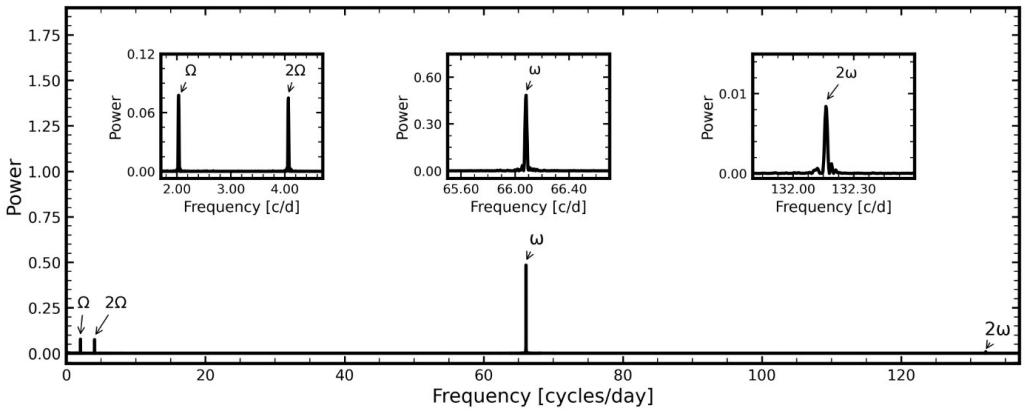

Figure 3: Lomb–Scargle periodogram of the TESS photometric light curve obtained during Sectors 88 and 89. The symbols Ω and 2Ω denote the binary orbital frequency and its first harmonic, respectively, while ω and 2ω represent the spin frequency of the white dwarf and its first harmonic. Adopted from figure 2 of [20].

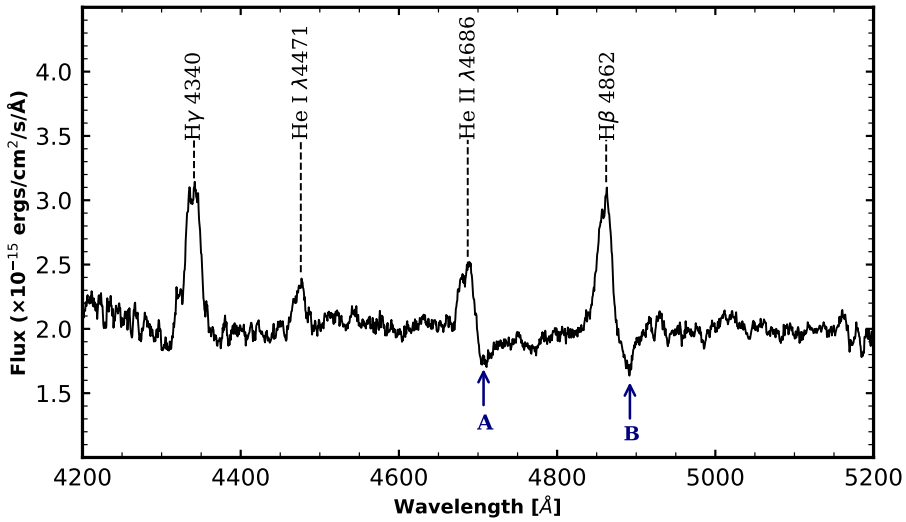

Figure 4: Average optical spectrum of 1RXS J080114.6–462324 obtained with the SAAO 1.9-m telescope in 2017 April 3. The prominent emission lines are identified. Arrows A and B mark the redshifted absorption dips following the He II λ4686 and Hβ emission lines, respectively.

3.3 Photopolarimetry

Figure 5 presents the photopolarimetric observations of 1RXS J080114.6–462324. The second and third panels of Figure 5 show clear evidence of circular and linear polarisation originating from the accretion regions of the WD. We report circular polarisation reaching approximately +5%, placing this system among the IPs exhibiting strong circular polarisation emission [23, 25]. The spin phase-folded light curve shown in Figure 6 indicates that the emission is modulated at the spin period of the accreting WD.

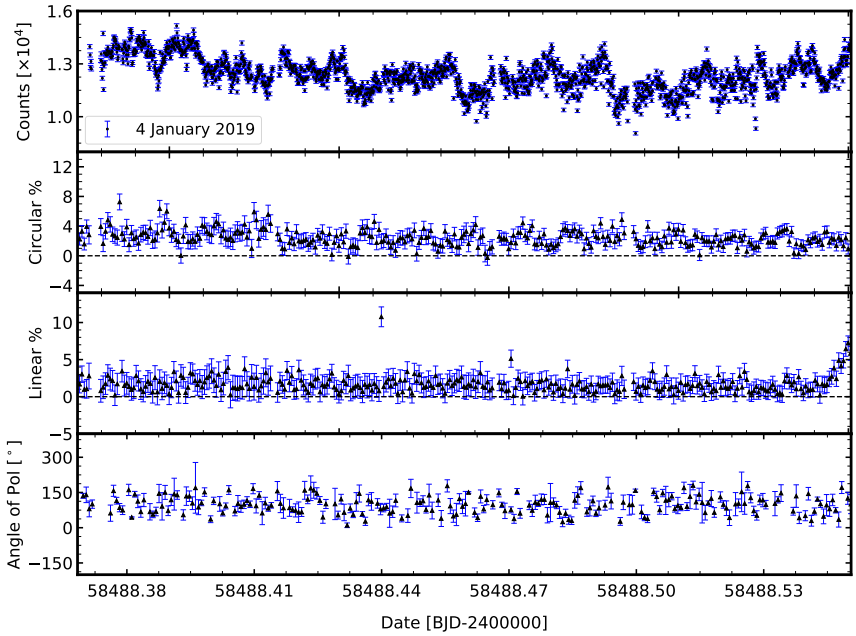

Figure 5: Optical photometric and polarimetric observations of 1RXS J080114.6–462324 obtained on 2019 January 4 using a clear filter. **Top panel:** Photometric light curve. **Second panel:** Circular polarisation percentage. **Third panel:** Linear polarisation light curve. **Bottom panel:** Position angle. Adopted from figure 12 of [20]

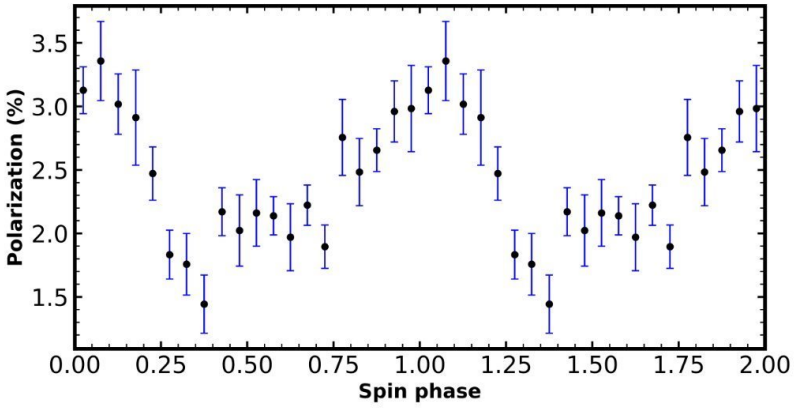

Figure 6: Spin-phase-binned circular polarisation light curve of 1RXS J080114.6–462324. Adapted from figure 7 of [20].

3.4 Circular Spectropolarimetry

The left and right panels of Figure 7 present the spin-phase-resolved circular spectropolarimetry observations of 1RXS J080114.6–462324 obtained on 2025 January 21, centered at spin phases ($\phi = 0.312$) and ($\phi = 0.816$), respectively. In both figures, the top panels show the average optical spectra, which exhibit typical emission lines associated with the accretion process, including the hydrogen Balmer series (Hδ to Hα) and several helium lines. The middle panels display clear detections of circular polarisation, slightly below +6% at phase ($\phi = 0.312$) and slightly above

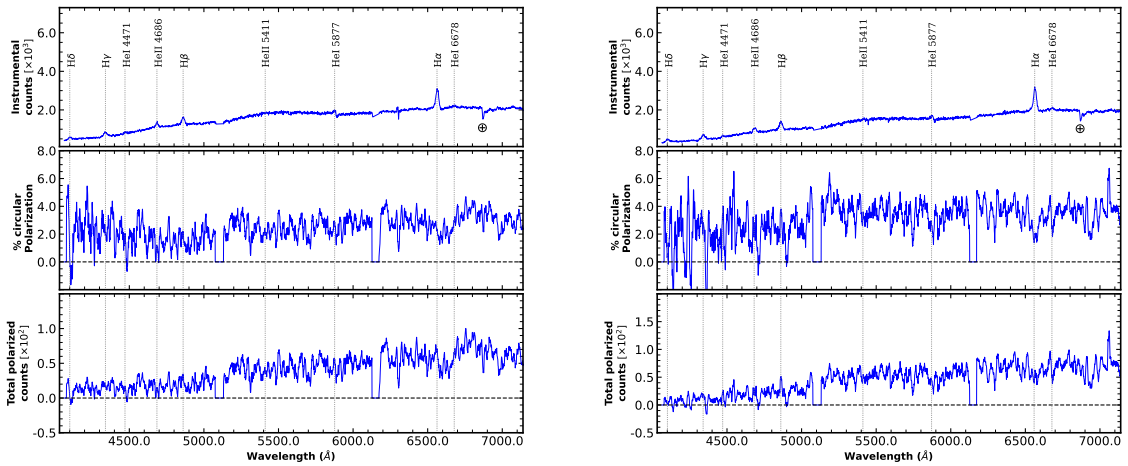

Figure 7: Optical circular spectropolarimetry of 1RXS J080114.6–462324 obtained on 2025 January 21, centered on the spin phase $\phi = 0.312$ (left panel) and $\phi = 0.816$ (right panel). **Top panel:** Optical spectrum with the principal emission lines identified; the symbol ⊕ marks regions affected by atmospheric absorption. **Middle panel:** Circular polarisation percentage spectrum. **Bottom panel:** Total polarised flux. In all panels, the dips around 5100 Å and 6150 Å correspond to the CCD chip gaps.

+6% at phase ($\phi = 0.816$). The observed differences in the polarisation spectra between these two phases are consistent with spin-modulated circular polarisation. We also note the absence of distinct cyclotron humps in the spectra, suggesting an upper limit of approximately 10 MG for the WD's surface magnetic field.

4. Discussion and Conclusion

This work has presented multi-technique observations of 1RXS J080114.6–462324, this includes photometry, spectroscopy, polarimetry and circular spectropolarimetry. This presents the first polarimetry observations of this system.

The TESS photometric light curves enabled us to detect the long binary orbital period, which was not possible with our SAAO 1.9-m telescope observations due to the short observational baseline. The detected orbital period of 11.8027 ± 0.0004 hours places our target among the intriguing group of IPs known to possess long binary orbital periods. Studying these systems is particularly valuable for understanding the evolutionary transition from long-period to short-period IPs. A comparable system is V2731 Oph [25], which shows circular polarisation varying between approximately −4% and +4.26%, and has a binary orbital period of 15.42 hours. Investigating systems with longer orbital periods provides valuable insight into how they evolve into shorter-period IPs such as EX Hydrae [26, 28].

The observed emission lines in the spectra of 1RXS J080114.6–462324 are generally consistent with those reported in [29]. However, in our data we also detect red-shifted absorption dips adjacent to HeII λ4686 and Hβ. We attribute these features to absorption by the accretion curtain as the WD rotates in and out of view. These spectral differences may reflect a different accretion state of the

system, highlighting the need for time-resolved optical spectroscopy to fully characterise the nature and variability of these features.

Our photopolarimetric and circular spectropolarimetric observations reveal a clear detection of circular polarisation in 1RXS J080114.6-462324. This constitutes the first direct evidence for a magnetic WD in this system. The phase dependence of the detected polarisation strongly indicates that it originates from the WD's accretion regions. The absence of cyclotron humps in the spectrum suggests an upper limit of $\lesssim$ 10 MG for the WD surface magnetic field.

5. ACKNOWLEDGEMENTS

The authors sincerely express their gratitude to the organisers for the kind invitation to participate in the HEASA 2025 conference, and to the reviewer for their valuable and insightful comments. This study makes use of data obtained with facilities at the South African Astronomical Observatory (SAAO), including the SAAO 1.0-m and 1.9-m telescopes, as well as the Southern African Large Telescope (SALT). Circular spectropolarimetric data were obtained under program 2024-2-SCI-038 (PI: Z. N. Khangale). We acknowledge financial assistance from the National Research Foundation (NRF) and National Astrophysics and Space Science Programme (NASSP). The financial assistance of the South African Radio Astronomy Observatory (SARAO) towards this research is hereby acknowledged (www.sarao.ac.za). This study also makes use of TESS data, which are publicly available from MAST.

References

[1] B. Warner, 1995, Cambridge Astrophysics Series, Vol. 28, Cambridge University Press, Cambridge

[2] C. Hellier, 2001, Cataclysmic Variable Stars, Springer-Verlag, London

[3] M.G. Watson, 1986, , eds. K. O. Mason, M. G. Watson, N. E. White, Vol. 266, p. 97, Springer-Verlag, Berlin, Heidelberg, doi:10.1007/3-540-17195-9_6

[4] B. Warner, 1992, Intermediate Polars and DQ Herculis Stars, ed. N. Vogt, ASP Conf. Ser., Vol.29, p.242

[5] J. Patterson, 1994, The DQ Herculis Stars, PASP, 106, 209, doi:10.1086/133375

[6] D. A. H. Buckley et al.,1995, MNRAS, 275, 1028-1048, doi:10.1093/mnras/275.4.1028

[7] A. J. Norton et al., 2008, ApJ, 672, 524–530, doi:10.1086/523932

[8] M. Cropper, 1990, SSRv, 54, 195–295, doi:10.1007/BF00177799

[9] L. A. Crause et al., 2016, Proc. SPIE, 9908, 990827, doi:10.1117/12.2230818

[10] L. A. Crause et al., 2019, JATIS, 5, 024007, doi:10.1117/1.JATIS.5.2.024007

[11] D. Tody, 1986, Proc. SPIE, 627, 733, doi:10.1117/12.968154

[12] S. B. Potter et al., 2010, MNRAS, 402, 1161–1170, doi:10.1111/j.1365-2966.2009.15944.x

[13] K. H. Nordsieck et al., 2003, Proc. SPIE, 4843, 170–179, doi:10.1117/12.459288

[14] K. H. Nordsieck, 2012, AIP Conf. Proc., 1429, 248–251, doi:10.1063/1.3701934

[15] S. B. Potter et al., 2016, Proc. SPIE, 9908, 99082K, doi:10.1117/12.2232391

[16] Z. A. Irving et al., 2024, MNRAS, 530, 3974–3985, doi:10.1093/mnras/stae1103

[17] F. Bernardini et al., 2017, MNRAS, 470, 4815–4837, doi:10.1093/mnras/stx1494

[18] J. P. Halpern et al., 2018, AJ, 155, 247, doi:10.3847/1538-3881/aabfd0

[19] A. Bruch, 2025, ApJS, 279, 48, doi:10.3847/1538-4365/addf41

[20] V. Moloi et al., 2025, MNRAS, 544, 1146–1159, doi:10.1093/mnras/staf1805

[21] A. J. Norton et al., 2004, ApJ, 614, 349–357, doi:10.1086/423333

[22] N. R. Lomb, 1976, APSS, 39, 447–462, doi:10.1007/BF00648343

[23] W. R. Penning et al., 1986, ApJ, 301, 881, doi:10.1086/163952

[24] J. D. Scargle, 1982, ApJ, 263, 835–853, doi:10.1086/160554

[25] O. W. Butters et al., 2009, A&A, 496, 891–902, doi:10.1051/0004-6361/200811058

[26] J. E. Pringle, 1975, MNRAS, 170, 633, doi:10.1093/mnras/170.3.633

[27] I. J. Lima et al., 2025, ApJ, 984, 152, doi:10.3847/1538-4357/adc380

[28] V. Suleimanov, V. Doroshenko, L. Ducci, G. V. Zhukov, and K. Werner, 2016, A&A, 591, A35, doi:10.1051/0004-6361/201628301

[29] N. Masetti et al., 2010, A&A, 519, A96, doi:10.1051/0004-6361/201014852